Spectrochimica Acta Part A: Molecular and Biomolecular Spectroscopy 284 (2023) 121756

Contents lists available at ScienceDirect

Spectrochimica Acta Part A:
Molecular and Biomolecular Spectroscopy

journal homepage: www.journals.elsevier.com/spectrochimica-acta-part-a-molecular-and-biomolecular-spectroscopy

New europium-doped carbon nanoparticles showing long-lifetime photoluminescence: Synthesis, characterization and application to the determination of tetracycline in waters

M.E. Pacheco [a], Ch. Chimeno-Trinchet [b], A. Fernández-González [b], R. Badía-Laíño [b,*]

[a] Laboratorio de Investigación y Desarrollo de Métodos Analíticos (LIDMA), Facultad de Ciencias Exactas, Universidad Nacional de La Plata, 47 y 115, 1900 La Plata, Argentina
[b] Department of Physical and Analytical Chemistry, Faculty of Chemistry, University of Oviedo Av., Julián Clavería 8, 33006-Oviedo, Spain

HIGHLIGHTS

- Europium-doped carbon nanoparticles were synthetized and characterized.
- Delayed photoluminescence of europium-doped carbon nanoparticles was studied and its behavior in different environments was evaluated.
- A tetracycline photoluminescent sensor was developed.
- An efficient and synergistic sensitization of europium photoluminescence was achieved by means of the simultaneous presence of carbon nanoparticles and tetracycline.
- Tetracycline analytical determination was performed in natural waters.

GRAPHICAL ABSTRACT

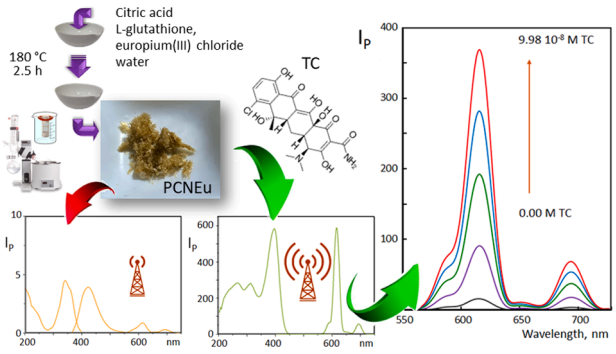

ARTICLE INFO

Keywords:
Carbon nanoparticles
Tetracycline
Europium
Natural water
Carbon dots

ABSTRACT

The growing appearance of antibiotic-resistant strains of microorganisms originated from the widespread use and ubiquitous presence of such drugs is a major concern in the world. The development of methodologies able to detect such substances at low concentration in real water samples is mandatory to overcome this problem. Europium(III) is known to form complexes with tetracycline (TC) with photoluminescent characteristics useful for TC determination.

In the present work, we synthesized for the first time carbon nanoparticles (CN) showing delayed photoluminescence using a Europium(III) doping synthesis. The new material (PCNEu) was characterized both morphologically and spectroscopically, showing an analytical photoluminescent signal in presence of TC, arising from the $^5D_0 \rightarrow {}^7F_2$ transition of europium, one hundred times higher than that of the europium salt alone in presence of the antibiotic. This enhancement is a consequence of the amplifying effect exerted by nanoparticle structure itself, leading to an efficient synergistic "antenna effect" in the system PCNEu - TC. The analytical signal is affected both by pH and the nature of the buffer used, and it allows the detection of tetracycline in waters with a limit of detection of 2.18 nM and recoveries between 90 and 110%. The analytical performance of the

* Corresponding author.
E-mail address: recomol@uniovi.es (R. Badía-Laíño).

https://doi.org/10.1016/j.saa.2022.121756
Received 10 May 2022; Received in revised form 22 July 2022; Accepted 10 August 2022
Available online 23 August 2022

developed methodology enables having lower limits of detection than other luminescent and chemiluminescent reported methodologies.

1. Introduction

The presence of antibiotics in waters is a growing issue, whose control becomes particularly important due to the long-term impact that could have on the environment. In fact, it is not infrequent to find in rivers, lakes, or phreatic waters such substances or their metabolites, some of which may still be active [1]. A higher consumption of pharmaceutical drugs, the concentration effect in hospital areas and in sewage muds as well as the increase of their use in veterinary and cattle raising, mainly as fattening agents, have favoured the appearance of such compounds at trace levels even in waters for human consumption or natural water sources distant from human settlements.

Antibiotics belonging to the tetracycline family may have both natural and synthetic origins, being the latter more stable and, thus, with a potentially higher environmental impact [2]. They have a bacteriostatic mechanism as they inhibit bacterial protein synthesis and they are active against Gram+ and other microorganisms [3,4]. After human consumption, many of them are eliminated without metabolic transformations, merging then with the antibiotics directly spilt in the environment, where they accumulate. Social sensitiveness about the environmental effect and the repercussions that these facts bring to health makes necessary the development of sensitive, fast and cheap methodologies to detect the presence of such substances in environmental samples.

In recent years, carbon nanoparticles (CNs) have attracted strong interest from the scientific community. These materials combine interesting properties such as photoluminescence, chemo- and photostability, high solubility in water, ease of synthesis, and surface functionalization with some biologically compelling properties like biodegradability, low toxicity, and scarce environmental impact [5-7]. Particularly, the unique optic and spectroscopic characteristics offered by these materials make them a powerful alternative in many applications such as optoelectronic labelling [8,9], bioimaging [6,10] or chemosensor development [11,12], among others.

On the other hand, it is well known that photoluminescent complexes of lanthanoids have been widely used as fluorescent probes in technological and bioanalytical applications [13]. Specifically, the Eu (III)-tetracycline complex (EuTC) [14] offers interesting photoluminescence features since its emission bands are narrow and at long wavelengths, it has a long Stokes shift and its photoluminescence lifetime is long too [15,16]. This latter property is very interesting for photoluminescent analytical applications, since recording long-delayed emission, typically in the milli or micro seconds range, minimizes or even minimizes the influence of potential interferences coming from fluorescent species, whose lifetime commonly lay within the nanosecond range. Additionally, EuTC complexes have been used to obtain interesting information about stability constants, energy-transfer efficiency and relative distance between fluorescent carbon nanoparticles and EuTC complex, helping so to understand the mechanisms originating the photoluminescent phenomena observed in the photoluminescent CNs [16]. Nevertheless, up to date and to our knowledge, long-lifetime Eu doped CNs have not been reported yet.

According to our previous experience and good results with glutathione and citric-acid based carbon dots for evaluating the interaction of tetracycline and europium complexes [16], we faced the challenge of 'doping' this kind of carbon dots with europium salts in order to obtain photoluminescent carbon nanoparticles containing europium (PCNEu) with delayed photoluminescence, so as to use them as nanochemosensors in the determination of tetracycline antibiotics in waters.

2. Experimental

2.1. Reagents, materials and solutions

Citric acid monohydrate 99%, L-Glutathione > 98% (GSH) and 2-amine-2-(hydroxymethyl)-1,3-propanediol hydrochloride > 99.8 % (TRIS) were purchased to Sigma-Aldrich; Europium(III) chloride hexahydrate 99.99% and Tetracycline hydrochloride > 98% (TC·HCl) were purchased from ACROS and Tokyo Chemical Industry CO., respectively. All chemicals were of analytical grade and used without further purifications. All the solutions were prepared using Milli-Q water (MQW). Standards TRIS buffer solution 1 M pH 6.0–8.5 and tetracycline (TC) $2.25{\cdot}10^{-4}$ M were prepared. The different solutions used in the study were prepared by dilution of both. All the solutions were kept in dark and at 4 °C when not used and freshly prepared every week. The purification of the nanoparticles was performed by dialysis with Pur-A-Lyzer Mega 1000 membranes from Sigma-Aldrich. Membranes were hydrated and stabilized in MQW for two hours previously to their use.

2.2. Instrumentation

The morphological and size evaluation of the nanoparticles was carried out with the images taken in a JEOL JEM-2100F high resolution transmission electron microscope operated at 200 kV. The device was equipped with an ultra-high resolution pole-piece providing a spatial resolution down to 0.19 nm, an X-ray detector of dispersive energy (EDX, instrument from Oxford INCA Energy TEM 250) for elemental microanalysis and a STEM (Gatan) control unit with a CCD camera (14-bit Gatan Orius SC600) and bright-field (BF) and HAADF detectors from JEOL.

The obtaining of the TEM images was as follows: an ethanolic dispersion of the nanoparticles sample was sprayed on a copper grid coated with carbon, air-dried and finally plasma-cleaned in a SOLARUS 950 Advanced Plasma Cleaning system before being loaded in the microscope. The mean size of the nanoparticles was estimated from the digitized images using ImageJ free software tool, making at least 150 observations for every dimension.

UV–Visible spectra were recorded in a Cary 60 UV–Vis from Agilent Technologies using 1x1x4 cm quartz cuvettes.

Photoluminescence spectra of nanoparticle suspensions were performed in a Varian Cary Eclipse from Agilent Technologies, equipped with a pulsed Xe lamp (2 μs half-width, 80 Hz) and a R928 photomultiplier tube. Steady-state photoluminescence measurements were carried out at room temperature, setting excitation and emission bandwidths at 5 nm unless otherwise stated. Delayed photoluminescence measurements in 1x1x4 cm quartz cuvettes and 96-well plates were performed setting the excitation and emission bandwidths at 20 nm, and the selected delay and gate times (specific conditions are mentioned in each experiment). *Delay time* refers to the elapsed time occurring from the excitation pulse and the starting time of recording the emission; *gate time* refers to the time during which the photodetector is capturing the emitted light, a kind of integration time.

Photoluminescence characterization and lifetimes of solids and dispersions were evaluated in an Edinburgh Instruments FS5 equipped with a 150 W Xenon lamp, a 5 W micropulsed Xe flash lamp for delayed photoluminescence measurements (<10 μs to >10 s) and a R928P photomultiplier tube. The photoluminescence of the solid $EuCl_3{\cdot}6H_2O$ salt was also evaluated with the same device, although it was diluted in anhydrous KBr in order to avoid the saturation of the detector.

Lyophilization was carried out in a Telstar CRYODOS.

2.3. Synthesis of photoluminescent carbon nanoparticles doped with Europium, PCNEu

Carbon nanoparticles doped with Europium, PCNEu, were obtained through a thermal carbonization procedure using a porcelain crucible in a conventional oven at 180 °C. The protocol of synthesis was as follows: 1 g citric acid, 0.5 g glutathione, and the proper amount of europium chloride hexahydrate were mixed together and solved into 5 mL MQW until obtaining a transparent solution. The solution was poured into a porcelain crucible and put into an oven at 180 °C for 2.5 h. During this time, aliquots of 1 mL MQW were regularly added to the solution every 30 min in order to avoid the product to scorch. The product was a brownish gel, which was re-suspended in 15 mL MQW and purified by dialysis against MQW for 24 h. The water of the purified suspension was removed by rota-evaporation and lyophilization. The final product was a dry brownish-green solid with a fibrous appearance, which was kept in dark at 4 °C until further use.

2.4. Analytical performance

2.4.1. Analytical calibration

A calibration curve for the determination of tetracycline in water was carried out in 0.1 M TRIS buffer (pH 8.5) with a fixed amount of 10 $\mu g \cdot mL^{-1}$ PCNEu and growing amounts of TC in the concentration range of $0.00–1.00 \cdot 10^{-7}$ M for standard quartz cuvette and $0.00–1.04 \cdot 10^{-6}$ M for 96-well plate reader configurations. Photoluminescence measurements were performed setting the excitation and emission wavelengths at 394 nm and 616 nm, respectively, with a delay time of 0.1 ms and a gate time of 2.5 ms. Figures of merit of the proposed analytical methodology were evaluated.

2.4.2. Analysis of tetracycline in real water samples

Natural water samples were taken in amber-coloured bottles and kept refrigerated during transportation and storage until the analysis. The tap water sample was taken in the laboratory itself prior to the measurement, after letting water flow for 3 min. All the samples were filtrated through a 0.25 μm filter before taking the aliquot.

TC was not detected in water samples and, therefore, a recovery study was performed by spiking the samples with different concentrations of TC. Spiked samples, at two different concentrations of TC, were prepared into 10.0 mL volumetric flasks (for standard cuvette assays) following the same procedure as in the calibration curve: a proper aliquot of PCNEu suspension, TC, MQW or sample and TRIS 1 M (pH 8.5) were added to the volumetric flask and brought to volume with MQW. Final concentrations of PCNEu, TC and TRIS were 10 $\mu g \cdot mL^{-1}$, $7 \cdot 10^{-9}$ M or $6 \cdot 10^{-8}$M, and 0.1 M, respectively. For 96-well plate reader measurements, the spiked TC final concentration was $6.24 \cdot 10^{-7}$ M (all other concentrations remain the same). The analysis was performed by adding the proper volumes to each well, being the final volume 250 μL. Sample dilution was 1/2 in each case. All analyses were performed in triplicate. The TC concentration was quantified by external calibration (Section 2.4.1.).

3. Results and discussion

3.1. Synthesis and characterization of PCNEu

The thermal oxidation of the chemical precursors used to obtain the PCNEu, citric acid and GSH, allows obtaining multifunctionalized nanoparticles with different surface functional groups (–COOH, –OH and $–NH_2$) [16] whereas the europium salt present during the synthesis incorporates metallic cations to the CN structure, yielding nanoparticles with an intense delayed photoluminescence emission.

In order to optimize the amount of doping salt, three different $EuCl_3 \cdot 6H_2O$ percentages were tested during the synthesis, 4.2%, 11.8% and 25.0% w/w, corresponding to 1.7%, 4.9% and 10.4% of lanthanoid ion w/w. Concentrations below 4.9% Eu(III) showed poor long-lifetime photoluminescence intensity whereas higher concentrations yielded a white precipitate during the purification process, probably arising from an excess of salt, as the higher the salt concentration the greater the amount of precipitate. Taking all of this into account, a 4.9% Eu(III) percentage was selected for further studies. Notwithstanding, semi-quantitative EDX analyses revealed a true 1.6 ± 0.5 Eu (III)% w/w (0.16 ± 0.04 % in atomic percentage) instead.

The shape and structure of PCNEu were evaluated with HRTEM, revealing that nanoparticles are mainly spherical with a 2.3 ± 0.7 nm diameter, as shown in Fig. 1. Fig. 1b shows clearly an inner structure with regularly-spaced layers with ca. 2 Å interlayer distance, which is significantly shorter than that for [0,0,2] layers of graphite [17]. This fact suggests a stronger interaction between the layers with an intermediate $sp^2–sp^3$ hybridization.

UV–vis absorption spectra of buffered aqueous suspensions of the synthesized PCNEu show the characteristic band of $\pi \rightarrow \pi^*$ transitions from C–C bonds in sp^2 hybridization at 240 nm overlapped with a different band at 347 nm attributable to $n \rightarrow \pi^*$ transitions from C=O bonds (yellow line in Fig. 2). In presence of tetracycline, UV–vis absorption spectra of PCNEu corresponding to 4.9% and 10.4% Eu(III) show an appreciable formation of Eu-TC complex between 375 and 425 nm (Fig. 2b-c). This result supports the selection of a 4.9% Eu(III) percentage in PCN.

The photoluminescence of the lyophilized PCNEu in solid-phase reveals an emission of very intense and narrow bands characteristic of the lanthanoids overlapped to a broad background emission when the excitation wavelength is 340 and 390 nm (Fig. 3). This emission spectrum coincides with the own photoluminescent emission of Eu^{3+} ions [18]. The strongest signal observed at 617 nm belongs to the so-called *induced electric dipole* (ED) transition, $^5D_0 \rightarrow {}^7F_2$, and it is responsible for the typical red photoluminescence, which can be observed in some compounds with Eu^{3+} [19,20]. This transition is also called "*hypersensitivity transition or pseudo-quadrupole transition*" because it depends on the Eu^{3+} ion symmetry and the nature of the ligands, unlike other ED transitions [18]. The presence of the two components of this band in the $EuCl_3 \cdot 6H_2O$ diluted in KBr spectrum indicates a D_3 symmetry for the metal ion [20], which is kept in the lyophilized PCNEu, although as non-resolved components in a broad band. The background emission corresponds to the own photoluminescence of lyophilized carbon nanoparticles (CNs), centered at around 560 nm (Fig. 3).

Regarding the photoluminescence of the aqueous buffered dispersions of PCNEu, they show a contrasting behaviour to that of the lyophilized material. The suspensions show broad excitation and emission bands centered respectively at 346 nm and 421 nm (Fig. 4a), and the emission corresponding to the europium ion is not observed. Thus, the emission band corresponding to the CNs in the aqueous buffered suspension of PCNEu appears approximately 139 nm blue-shifted, in respect of the lyophilized PCNEu, which is an indication of the destabilization of the nanostructure (enlargement of the band gap) due to the presence of water in the system. The wavelengths observed in this case are the characteristic ones of the CNs photoluminescence, resulting from the passivation process, which takes place during the synthesis. These CNs photoluminescence wavelengths do not change with the excitation energy used nor with the particle size and coincide with those obtained from the same precursors reported by Díaz-Faes López et al. for CNs but with a mean diameter 10 times bigger [16], and by Chimeno et al. for CNs with diameters in the 2–3 nm range with and without surface functionalization [21]. Additionally, the delayed photoluminescence also exhibits those broad bands centered at 346 nm (excitation) and 421 nm (emission), remarkably diminished, and the characteristic emission bands of europium ion (Fig. 4b). The extremely weak delayed emission observed at the wavelengths corresponding to the europium ion in an aqueous buffered medium agrees with the expectations since photoluminescence of lanthanoids is highly sensitive to the presence of water molecules [22], which induces the attenuation of the emission of the

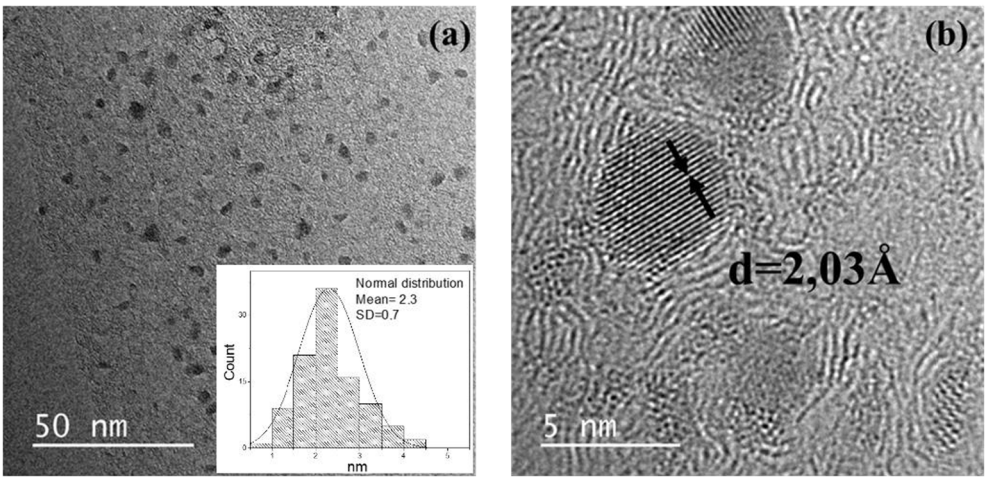

Fig. 1. HRTEM images for PCNEu. Inset shows size histogram for PCNEu.

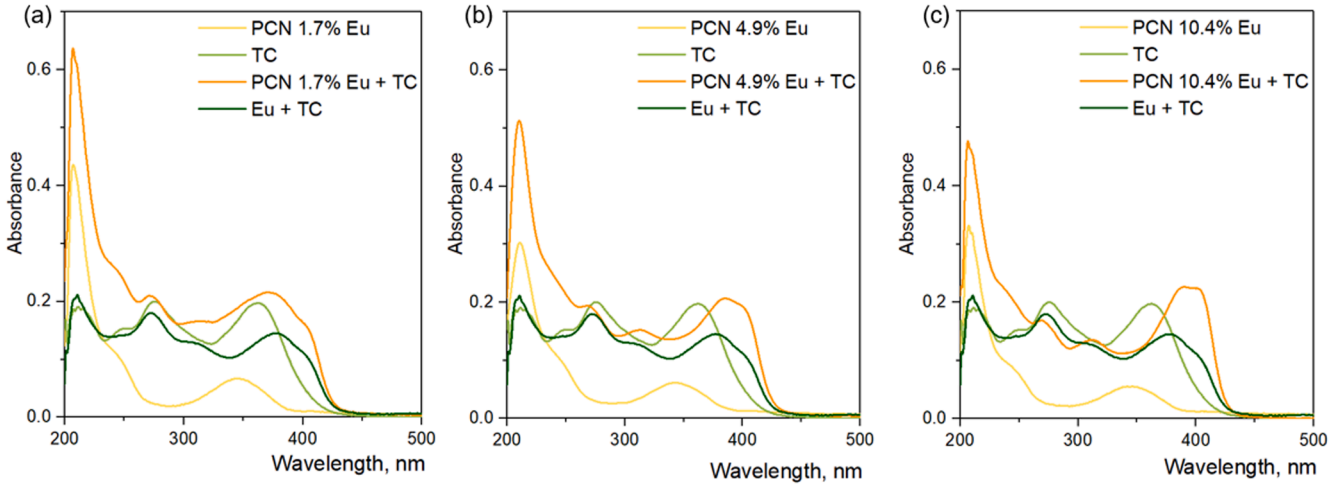

Fig. 2. UV–vis absorption spectra of PCNEu synthesized with different percentages of Eu(III), in the absence and presence of tetracycline (TC). UV–vis absorption spectra of $EuCl_3{\cdot}6H_2O$ in presence of TC is also shown for comparison. (a) 1.7% Eu(III), (b) 4.9% Eu(III), (c) 10.4% Eu(III); buffer Tris 0.1 M pH 7.4; 11 ppm PCNEu; $1{\cdot}10^{-5}$ M TC; 1.3 ppm $EuCl_3{\cdot}6H_2O$.

doping ion present in the nanoparticles, indicating that the water molecules have easy access to the environment of the metal ion.

Concerning the lifetimes of the delayed photoluminescence recorded in Table 1 for PCNEu, the presence of two long-terms suggests the existence of two different environments for europium ion in the CN: the longest component (τ_2) can be attributed to the photoluminescence decay from Eu^{3+} ions located in a protected surround within the core of CN or Eu^{3+} ions partially hindered or blocked for interaction with the surroundings, while the shorter one (τ_1) can be attributed to the photoluminescence decay from more exposed Eu^{3+} ions located at or near the surface of the CN. In this sense, the drastic decrease in both long-term lifetimes for PCNEu in water, compared to lyophilized PCNEu, clearly demonstrates that the presence of water facilitates a nonradiative deactivation pathway due to vibronic coupling with O-H oscillator retreating the sensitization process. In an aqueous buffered medium, TRIS molecules can displace water molecules from the coordination sphere of europium leading to an enhancement of τ_2 (270 μs), which almost reaches the one reported for lyophilized PCNEu (300 μs), whereas the lower value for τ_1 (1.7 μs) possibly indicates that TRIS molecules could not completely displace water molecules from the surface of PCNEu and, thus, a considerable source of nonradiative deactivation is still present (reflected also in the low intensity values).

3.2. Interaction of PCNEu with tetracycline

It has been reported that the presence of certain antibiotics of the tetracycline family (tetracycline, chlortetracycline, doxycycline or oxytetracycline), are able to form coordination complexes with europium, activating the photoemission of the wavelengths of Eu^{3+} itself [23,24]. This activation phenomenon can be explained by taking into account that the coordination of the tetracyclines with europium displaces the water molecules coordinated to the Eu^{3+} ion, isolating, thus, the cation from their attenuating effect. Tetracyclines forming highly stable complexes with Eu^{3+} act as 'antennae' (sensitization) capturing the UV radiation and intramolecularly transferring it to the metal ion. Then, the high energy levels of the cation are easily populated, enabling the photoluminescence emission to occur [15,25].

Fig. 5 shows the photoemission at 616 nm (excitation 394 nm, 0.1 ms delay time, 2.5 ms gate time) of the system as a function of the amount of added tetracycline, revealing a direct proportionality. The corresponding emission of CNs at 421 nm remains almost invariable. Enhancement of the PCNEu photoluminescence was fast and sensitive, with a stable signal after 10 min of interaction with the tetracycline. Therefore, the TC has easy access to the environment of the Eu^{3+} and is able to displace water molecules from the coordination of the metal ion leading to an effective sensitization.

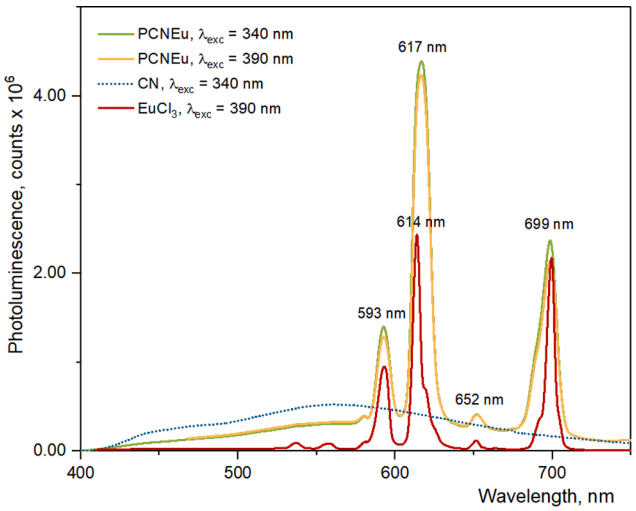

Fig. 3. (—) Photoluminescence of lyophilized PCNEu, excitation at 340 nm; (—) Photoluminescence of lyophilized PCNEu, excitation at 390 nm; (—) Photoluminescence of solid $EuCl_3$, excitation at 390 nm; (----) Photoluminescence of lyophilized carbon nanoparticles (CNs) synthetized with no addition of europium chloride hexahydrate, excitation at 340 nm.

Considering the long-lived photoluminescence lifetimes reported in Table 1, τ_1 for PCNEu-TC has a value of 79.6 μs, closer to the one observed for lyophilized PCNEu (106 μs). This could indicate that TC mostly resides on the surface of the PCNEu, resulting in a large shielding effect of Eu^{3+} ion. The lower value observed for τ_2 (174 μs) could be attributed to the additional sensitization process that involves the TC excited states. The interaction between TC and PCNEu can be understood as a ternary system CN-Eu-TC that exhibits a highly efficient "antenna effect" as a result of the shielding of Eu^{+3} ions environments from the potential quencher (O-H oscillator) and/or efficient intramolecular energy transfer from TC to Eu^{3+}.

In order to characterize the enhancing effect of the CN on the photoluminescence sensitivity of Eu^{+3} towards TC, a comparative study of the analytical signal using neat $EuCl_3{\cdot}6H_2O$ and PCNEu containing the same amount of Eu^{+3} ion as the salt was performed. The estimation of the amount of europium in the nanoparticles was achieved considering that the total amount of Eu^{+3} used in the synthesis was incorporated in the CNs. Fig. 6 shows the photoluminescence excitation and emission spectra of 11 ppm PCNEu and 1.3 ppm $EuCl_3{\cdot}6H_2O$ in the presence of TC 10^{-5} M in a pH 7.4 buffered medium. As can be seen there, PCNEu shows

Table 1
Long-lived photoluminescence lifetimes of PCNEu in different environments.

Lifetimes (μs)			
Material	**λ_{exc} - λ_{em} (nm)**	**τ_1**	**τ_2**
Lyophilized PCNEu	346–616	106 ± 2	300 ± 1
PCNEu in water	396–616	0.71 ± 0.02	9.0 ± 0.1
PCNEu in TRIS 0.1 M pH 8.5	396–616	1.7 ± 0.1	270 ± 2
PCNEu-TC in TRIS 0.1 M pH 8.5	396–616	79.6 ± 0.7	174 ± 1

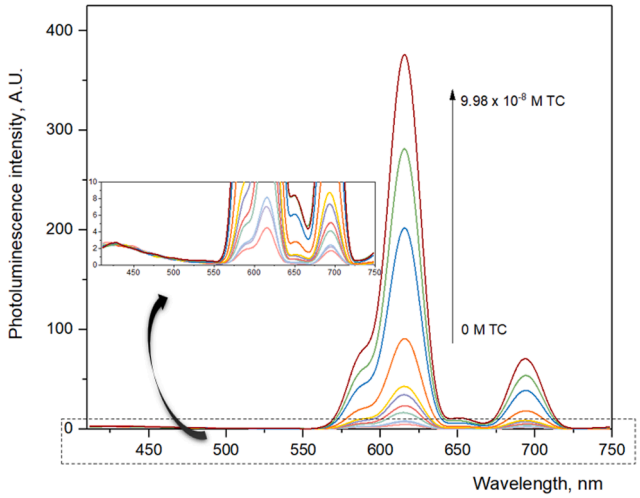

Fig. 5. Photoluminescence emission spectra of 10 ppm PCNEu in presence of different concentrations of TC; buffer Tris 0.1 M, pH 8.5; 394 nm excitation wavelength; delay time 0.1 ms and gate time 2.5 ms.

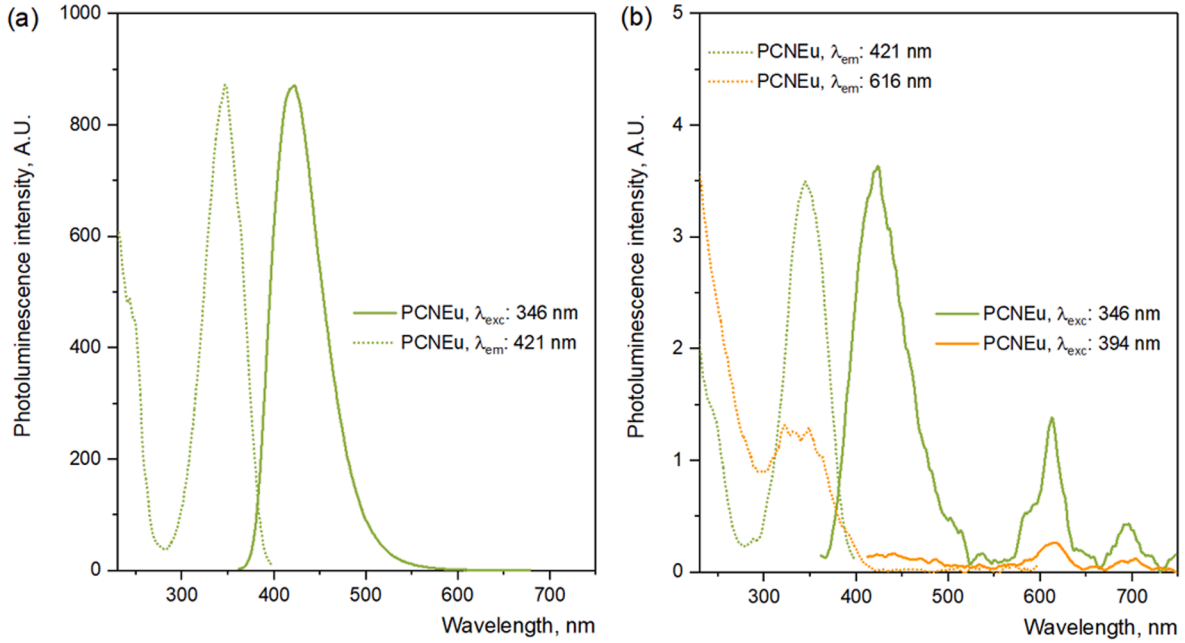

Fig. 4. (a) Photoluminescence excitation (dotted lines) and emission spectra (solid lines) of PCNEu in buffer Tris 0.1 M pH 7.4; (b) delayed photoluminescence excitation and emission spectra of PCNEu in buffer Tris 0.1 M pH 7.4, delay time 0.1 ms and gate time 5.0 ms.

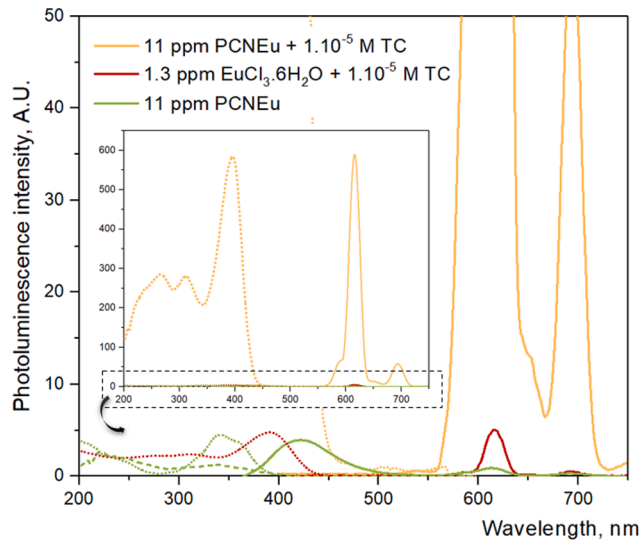

Fig. 6. (—) Photoluminescence excitation (λ_{em} 616 nm) and emission (λ_{exc} 394 nm) spectra of 11 ppm PCNEu (0.55 ppm Eu^{3+}) in presence of 1.10^{-5} M TC, and (—) 1.3 ppm $EuCl_3{\cdot}6H_2O$ (0.55 ppm Eu^{3+}) in presence of 1.10^{-5} M TC. (—) Photoluminescence excitation (λ_{em} 421 nm -dot-, 616 nm -short dash-) and emission (λ_{exc} 346 nm) spectra of 11 ppm PCNEu (0.55 ppm Eu^{3+}). Buffer Tris 0.1 M pH 7.4; delay time 0.1 ms and gate time 5.0 ms. Excitation spectra are plotted in dotted lines.

a 100-times more intense useful analytical signal than the neat salt. This fact is indicative of the amplifying effect exerted by nanoparticle structure itself on the Eu^{3+} emission, leading to an efficient synergistic "antenna effect".

The effect of pH and buffer nature played a critical role in the detection system of TC, as the antibiotic protonation limits the coordination capability of Eu^{3+}. As already mentioned, the incorporation of TC molecules within the coordination sphere of the metal ion removes the coordinated water molecules, which deactivate lanthanide photoluminescence and, therefore, enhances the sensitization rising the intensity of the photoemissive process. Since tetracycline is reported to have three different pK_a values, 3.3, 7.7 and 9.7 at 25 °C [26] belonging, respectively, to the tricarbonyl system, to the phenolic diketone system and to the ammonium cation, acid pH is expected to produce the lowest photoluminescence, as all the functional groups able to interact with the metal ion are protonated and, therefore, unable to react. At pH higher than 6.0, the groups able to interact with the metal ion begin to deprotonate (check pK_{a2} in Table 2). This is manifested through an analytically useful signal whose intensity depends on the nature of the buffer used. This is probably due to the competition established between the deprotonated groups of the TC and the anions of the buffer molecules themselves. Thus, when pH was buffered with PBS 0.1 M the photoluminescence was very weak and almost totally pH-independent (Fig. 7). This behaviour is due to the strong interaction between Europium(III) and phosphate anions, which cannot be disrupted by the tetracycline regardless of its deprotonation degree (see Table 2). When buffering with MOPS or TRIS, whose association constants are lower than that of TC and their concentration is 5 times more than TC, the emission intensity clearly depends on the pH and buffer nature, with the highest signal in both cases at pH 8.3 and very similar in value. This pH is higher than the pK_a of the hydroxyl groups responsible for the coordination of all the involved species. The one with the lowest pK_a, TRIS, is the first one in becoming incorporated into the coordination sphere, being gradually displaced by TC, showing the typical sigmoid response of titration with the titrating agent slowly aggregated. The concentration of deprotonated TC increases as the pH grows. In the case of MOPS, TC is gradually incorporated into the inner sphere of Eu^{3+}, showing a practically linear dependence of the signal with pH in the range of

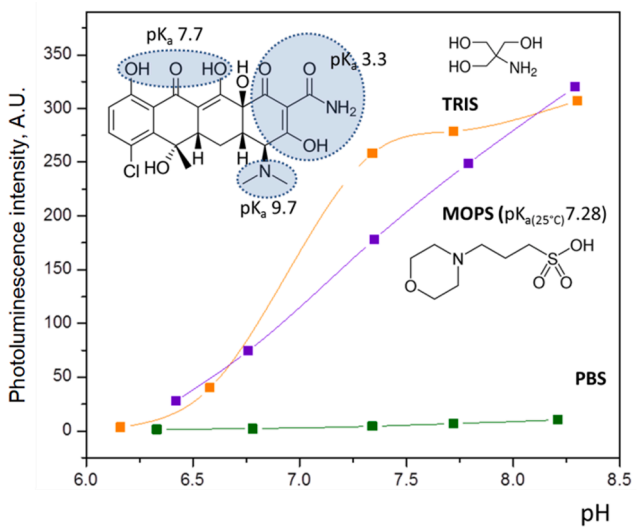

Fig. 7. pH and buffer nature (0.1 M) effect on PCNEu photoluminescence (10 ppm) in the presence of 10^{-6} M de TC; λ_{ex} 394 nm, λ_{em} 616 nm, delay time 0.1 ms, gate time 5.0 ms.

Table 2
pK_a and binding constants with europium for tetracycline, TRIS, MOPS and PBS.

Substance	Structure	pKa			Log K_f
		pKa_1	pKa_2	pKa_3	
Tetracycline	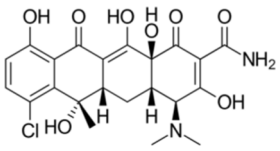	3.3	7.7	9.7	3.02 [27] $[Eu_3(TC)]^{3+}$
Tris	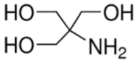	–	7.3	–	2.4 [28][Eu(*Tris*)]$^{3+}$
MOPS	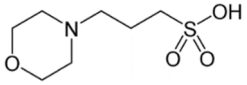		8.1		
PBS	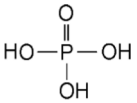	2.1	7.2	12.7	5.3[29]

6.5–8.3. In this interval, MOPS does not have the capability of displacing TC from the coordination sites even when pH grows over its pK_{a2} value (Fig. 7).

The interaction between the buffer 2-amino-2-(hydroxymethyl)propane-1,3-diol (*Tris*) and the Eu(III) ion has been studied by photoluminescence spectroscopy in D_2O. Emission and excitation spectra ($^5D_0 \leftarrow {}^7F_0$ transition) indicate an interaction with both $[TrisH]^+$ and neutral *Tris* species. The former is weak and probably of the outer-sphere type. The latter is of inner-sphere type and corresponds to the formation of the $[Eu(Tris)]^{3+}$ species (estimated $\log K_1 = 2.3 \pm 0.3$) [28]. Buffer *Tris* is also demonstrated to prevent the formation of an Eu-hydroxo species in the pD range of 7–8. Potentiometric measurements in H_2O allowed a more precise calculation of the stability constant: $\log K_1 = 2.44 \pm 0.07$ [28]. Comparison with the data for aliphatic amines and other metal ions leads to the conclusion that the Eu/*Tris* interaction is mainly achieved through the amino group. ^{1}H-NMR spectra in presence of Tb (III) ions confirmed both this assumption and the presence of a weak interaction with $TrisH^+$. Quantitative determinations of association constants between lanthanide ions and macromolecules of biological interest performed in presence of *Tris* should, therefore, be corrected for the Eu/*Tris* interaction.

The maximum photoluminescence effect took place in alkaline *Tris* media and a pH range from 7.3 to 8.5, which was selected as the optimum values for further experimental measurements.

The effect of PCNEu concentration on the analytical signal was also evaluated. In order to do that, two series of nanoparticle suspensions ranging from 0 to 20 ppm were prepared at two different tetracycline levels, $2.5{\cdot}10^{-7}$M and $2.5{\cdot}10^{-6}$M. In both cases, the analytical signal rises until reaching a plateau at 5 and 10 ppm respectively (Figure SI1). A PCNEu concentration of 10 ppm was selected for further studies.

3.3. Analytical figures of merit

The analytical figures of merit were evaluated according to the IUPAC recommendations [30-32]. External calibration curves (Figures SI2 and SI3) were prepared using 10 different standards with three replicates of each one. Table 3 summarizes both the analytical figures of merit as well as the optimal experimental conditions using either the standard cuvette-based assay or a 96-well plate reader. The limit of detection is comparable to other techniques requiring much more sophisticated protocols and devices, as shown in Table 4.

Table 3
Optimal condition and analytical figures of merit.

Optimal condition		
Instrumental	**λ excitation**	394 nm
	λ emission	616 nm
	Delay time, t_d	0.1 ms
	Gate time, t_g	2.5 ms
	Excitation/Emission Bandwidth	20 nm
Experimental	**Buffer**	Tris 0.1 M
	pH	8.5
	[PCNEu]	10 ppm
Analytical Figures of Merit		
Format	**Standard system**	**96 Well Plate Reader**
Calibration curve	$I_{pl} = (5 \pm 2) + (3.81 \pm 0.05)\ 10^9\ M^{-1}$ [TC] ($s_{y/x}$ 4; 95% confidence intervals for parameters; lack of fit: p-value = 0.4387)	$I_{pl} = (-3 \pm 8) + (5.7 \pm 0.2)\ 10^8\ M^{-1}$ [TC] ($s_{y/x}$ 19; 95% confidence intervals for parameters; lack of fit: p-value = 0.9299)
Analytical sensitivity, γ	$9.43{\cdot}10^8\ M^{-1}$	$3.06{\cdot}10^7\ M^{-1}$
LOD	2.18 nM	65 nM
LOQ	6.65 nM	200 nM
Dynamic range	$2.18{\cdot}10^{-9}$ M–$1.00{\cdot}10^{-7}$ M	$65{\cdot}10^{-9}$ M–$1.04{\cdot}10^{-6}$ M
Linear range	$6.65{\cdot}10^{-9}$ M–$1.00{\cdot}10^{-7}$ M	$200{\cdot}10^{-9}$ M–$1.04{\cdot}10^{-6}$ M

3.4. Proof of concept: Real sample analysis

In spite of existing a growing concern about the possibility of the evolution and spreading of antibiotic-resistant pathogens boosted by the presence of these drugs in the environment, there is no current regulatory system that takes into account such risks. This fact is partially due to the limited knowledge of the antibiotic concentrations which might lead to the selection of resistant bacteria. Nonetheless, it is usually considered that the maximum concentration of antibiotics should be lower than that able to inhibit completely the bacterial growth. In the case of tetracyclines, the minimum inhibition concentration (MIC) is estimated at 16 μg/L (36 nM) [36], whereas the Predicted No-Effect Concentration (PNEC) resulted to be 1 μg/L (2.5 nM).

In order to evaluate whether the developed methodology is applicable in this context, samples of natural waters were obtained from three different points in the Principality of Asturias: a stream in the route Taranes – Llambria, the river Trubia in the 'Senda del oso' and tap water from the Oviedo city. Samples were spiked with TC at two different levels: $7{\cdot}10^{-9}$ M and $6{\cdot}10^{-8}$M, and the individual recovery was evaluated in every case. The average recovery and its statistical 95% confidence interval were calculated for standard cuvette configuration (Table 5), thus confirming the applicability as a nanoprobe for antibiotic screening in natural and tap water, and its quantification over PNEC. In case of concentrations considerably higher than MIC, in the range of μM, as can be those from waste discharge or effluents [37], the use of a 96-well plate reader allows the simultaneous and fast evaluation of a high amount of samples in the different points with good recuperations (acceptable average recovery at 0.6 μM as shown in Table 5).

4. Conclusions

The synthesis of long-lifetime photoluminescent carbon nanoparticles doped with europium is reported for the first time. The new nanomaterials result in photoluminescent nanoparticles with an intermediate hybridization between sp^2 and sp^3, which not only keep the photoluminescent properties of both the carbon dots and the lanthanoid, with longer lifetimes, but also exerting an additional antenna effect on the ion.

The induced electric dipole transition at 617 nm of the Europium ion, $^5D_0 \rightarrow {}^7F_2$, is affected by the presence of tetracycline antibiotics by coordinating and displacing water molecules. This interaction can be exploited to determine the amount of this antibiotic in natural and tap water.

The incorporation of Europium within the CN structure resulted in a 100-times enhanced photoluminescence signal which drastically improves the analytical applicability of the system.

The analytical figures of merit of this methodology based on PCNEu show a limit of detection of $2.18{\cdot}10^{-9}$ M with an analytical sensitivity of $9.43{\cdot}10^8\ M^{-1}$, appropriated for its use as nanoprobe in natural and tap water.

Table 4
Comparison of the Limit of Detection.

Technique	**Type of sample**	**LOD / nM**	**Reference**
Chemiluminescence	Honey / drugs	30–100[†]	25
SPE-HPLC-MS	Water	0.03–0.2	[33]
Luminescence	Water / milk	15	[34]
DES-(ABA-DLLME)/HPLC-UV	Water	18	[35]
PCNEu photoluminescence	Water	2.18	This work

[†] Evaluated for chlortetracycline, oxytetracycline and doxycycline.

Table 5
Recoveries for TC determination in spiked natural and tap water (for simplicity, mean individual recoveries from triplicate assays are shown). Average recovery ($\overline{R}$) and its 95% confidence interval are included (homogeneity of variance between groups was tested).

Sample	Spiked concentration		
	Standard system		96 Well Plate Reader
	$7.00{\cdot}10^{-9}$ M	$6.00{\cdot}10^{-8}$ M	$6.24{\cdot}10^{-7}$ M
Taranes Stream–Llambria	102 %	103 %	109 %
Trubia River, Senda del Oso	99 %	98 %	91 %
Tap water in Oviedo	101%	104 %	94 %
$\overline{R} \pm t_{(0.025,N-1)}\frac{S_R}{\sqrt{N}}$	101 ± 3 % (N = 9)	101 ± 5 % (N = 9)	98 ± 8 % (N = 9)
	101 ± 3 % (N = 18)		

Declaration of Competing Interest

The authors declare that they have no known competing financial interests or personal relationships that could have appeared to influence the work reported in this paper.

Data availability

Data will be made available on request.

Acknowledgments

The authors gratefully acknowledge financial support from the Ministerio de Ciencia, Innovación y Universidades (MCIU), Agencia Estatal de Investigación (AEI) and European Regional Development Fund (FEDER), Project # RTI2018-099756-B-I00 (MCIU/AEI/FEDER, UE). MEP is member of the research career of CIC (Buenos Aires, Argentina).

Appendix A. Supplementary data

Supplementary data to this article can be found online at https://doi.org/10.1016/j.saa.2022.121756.

References

[1] M.-C. Danner, A. Robertson, V. Behrends, J. Reiss, Antibiotic pollution in surface fresh waters: Occurrence and effects, Science of the Total Environment 664, Sci. Total Environ. 664 (2019) 793–804.
[2] P. Chaturvedi, P. Shukla, B.S. Giri, P. Chowdhary, R. Chandra, P. Gupta, A. Pandey, Prevalence and hazardous impact of pharmaceutical and personal care products and antibiotics in environment: A review on emerging contaminants, Environ. Res. 194 (2021) 110664.
[3] S. Gaur, A. M Bal, Tetracyclines , Reference Module in Biomedical Sciences, Elsevier, 2021, ISBN 9780128012383; doi: 10.1016/B978-0-12-820472-6.00185-7.
[4] M. Roberts, Tetracycline resistance determinants: mechanisms of action, regulation of expression, genetic mobility, and distribution, FEMS Microbiol. Rev. 19 (1) (1996) 1–24.
[5] B. Wang, H. Song, X. Qu, J. Chang, B. Yang, S. Lu, Carbon dots as a new class of nanomedicines: Opportunities and challenges, Coordination Chem. Rev. 442 (2021) 214010.
[6] K.O. Boakye-Yiadom, S. Kesse, Y. Opoku-Damoah, M.S. Filli, M. Aquib, M. M. Bazezy Joelle, M.A. Farooq, R. Mavlyanova, F. Raza, R. Bavi, B. Wang, Carbon dots: Applications in bioimaging and theranostics, Int. J. Pharm. 564 (2019) 308–317, https://doi.org/10.1016/j.ijpharm.2019.04.055.
[7] N. Esfandiari, Z. Bagheri, H. Ehtesabi, Z. Fatahi, H. Tavana, H. Latifi, Effect of carbonization degree of carbon dots on cytotoxicity and photo-induced toxicity to cells, Heliyon 5 (12) (2019) e02940.
[8] F. Yan, H. Zhang, N. Yu, Z. Sun, L. Chen, Conjugate area-controlled synthesis of multiple-color carbon dots and application in sensors and optoelectronic devices, Sens. Actuators B: Chem. 329 (2021) 129263.
[9] X. Ren, W. Liang, P. Wang, C.E. Bunker, M. Coleman, L.R. Teisl, L.i. Cao, Y.-P. Sun, A new approach in functionalization of carbon nanoparticles for optoelectronically relevant carbon dots and beyond, Carbon 141 (2019) 553–560.
[10] Z. Peng, X. Han, S. Li, A.O. Al-Youbi, A.S. Bashammakh, M.S. El-Shahawi, R. M. Leblanc, Carbon dots: Biomacromolecule interaction, bioimaging and nanomedicine, Coordination Chem. Rev. 343 (2017) 256–277, https://doi.org/10.1016/j.ccr.2017.06.001.
[11] J. Espina-Casado, A. Fernández-González, M.E. Díaz-García, R. Badía-Laíño, Smart carbon dots as chemosensor for control of water contamination in organic media, Sensors and Actuators B: Chemical 329 (2021) 129262; doi:10.1016/j.snb.2020.129262.
[12] H.O. Othman, R.O. Hassan, A.T. Faizullah, A newly synthesized boronic acid-functionalized sulfur-doped carbon dot chemosensor as a molecular probe for glucose sensing, Microchemical Journal 163 (2021) 105919.
[13] M.L. Aulsebrook, B. Graham, M.R. Grace, K.L. Tuck, Lanthanide complexes for luminescence-based sensing of low molecular weight analytes, Coordination Chem. Rev. 375 (2018) 191–220, https://doi.org/10.1016/j.ccr.2017.11.018.
[14] L.M. Hirsch, T.F. Van Geel, J.D. Winefordner, R.N. Kelly, S.G. Schulman, Characteristics of the binding of europium(III) to tetracycline, Anal. Chimi Acta 166 (1985) 207–219, https://doi.org/10.1016/S0003-2670(00)84868-0.
[15] J. Georges, S. Ghazarian, Study of europium-sensitized fluorescence of tetracycline in a micellar solution of Triton X-100 by fluorescence and thermal lens spectrometry, Anal. Chim. Acta 276–2 (1993) 401–409, https://doi.org/10.1016/0003-2670(93)80411-D.
[16] T. Díaz-Faes López, A. Fernández González, M.E. Díaz-García, R. Badía-Laíño, Highly efficient Förster resonance energy transfer between carbon nanoparticles and europium–tetracycline complex, Carbon 94 (2015) 142–151, https://doi.org/10.1016/j.carbon.2015.06.066.
[17] P.L. Walker, H.A. McKinstry, C.C. Wright, X-Ray Diffraction Studies of a Graphitized Carbon, Ind. Eng. Chem. 45 (1953) 1711–1715, https://doi.org/10.1021/ie50524a033.
[18] K. Binnemans, Interpretation of europium(III) spectra, Coordination Chem. Rev. 295 (2015) 1–45, https://doi.org/10.1016/j.ccr.2015.02.015.
[19] K. Wahid, M. Pokhrel, Y. Mao, Structural, photoluminescence and radioluminescence properties of Eu3+ doped La2Hf2O7 nanoparticles, J. Solid State Chem. 245 (2017) 89–97, https://doi.org/10.1016/j.jssc.2016.10.004.
[20] A.G. Bispo-Jr, G.M.M. Shinohara, A.M. Pires, C.X. Cardoso, Red phosphor based on Eu3+-doped Y2(MoO4)3 incorporated with AuNPs synthesized via Pechini's method, Opt. Mater. 84 (2018) 137–145, https://doi.org/10.1016/j.optmat.2018.06.023.
[21] C. Chimeno-Trinchet, M.E. Pacheco, A. Fernández-González, M.E. Díaz-García, R. Badía-Laíño, New metal-free nanolubricants based on carbon-dots with outstanding antiwear performance, J. Ind. Eng. Chem. 87 (2020) 152–161, https://doi.org/10.1016/j.jiec.2020.03.032.
[22] J.R. Lakowicz, Fluorophores in Principles of Fluorescence Spectroscopy, third ed., Springer, Singapore, 2006, ISBN-10: 0-387-31278-1.
[23] N. Arnaud, J. Georges, Sensitive detection of tetracyclines using europium sensitized fluorescence with EDTA as co-ligand and cetyltrimethylammonium chloride as surfactant, Analyst,126 (2001) 694-697; doi: 10.1039/B101525G.
[24] M. Kaczmarek, S. Lis, Chemiluminescence determination of tetracyclines using Fenton system in the presence europium(III) ions, Anal. Chim. Acta 639 (2009) 96–100, https://doi.org/10.1016/j.aca.2009.02.047.
[25] L.C. Courrol, R.E. Samad, Applications of Europium Tetracycline Complex: A Review, Curr. Pharm. Anal. 4 (2008) 238–248.
[26] Clarke's Isolation and Identification of Drugs, second ed., 1986, p. 1005.
[27] S.K. Ghorai, S.K. Samanta, M. Mukherjee, P. Saha Sardar, S. Ghosh, Swarna Kamal Samanta, Manini Mukherjee, Pinki Saha Sardar, and Sanjib Ghosh, Tuning of "Antenna Effect" of Eu(III) in Ternary Systems in Aqueous Medium through Binding with Protein, Inorg. Chem. 52 (3) (2013) 1476–1487.
[28] J.-M. Pfefferl, J.-C. Bünzli, Interaction between the buffer Tris and the Eu(III) ion: Luminescence and potentiometric investigation, Helvetica 72 (1989) 1487–1494, https://doi.org/10.1002/hlca.19890720709.
[29] N.a. Shao, J. Jin, G. Wang, Y. Zhang, R. Yang, J. Yuan, Europium(iii) complex-based luminescent sensing probes for multi-phosphate anions: modulating selectivity by ligand choice, Chem. Commun. (9) (2008) 1127.
[30] L.A. Currie, Nomenclature in evaluation of analytical methods including detection and quantification capabilities (IUPAC Recommendations 1995), Anal. Chim. Acta 391 (1999) 105–126, https://doi.org/10.1016/S0003-2670(99)00104-X.
[31] L.A. Currie, Detection and quantification limits: origins and historical overview, Anal. Chim. Acta 391 (1999) 127–134, https://doi.org/10.1016/S0003-2670(99)00105-1.
[32] A.C. Olivieri, Practical guidelines for reporting results in single- and multi-component analytical calibration: A tutorial, Anal. Chim. Acta 868 (2015) 10–22, https://doi.org/10.1016/j.aca.2015.01.017.
[33] H.-C. Ri, J. Piao, L. Cai, X. Jin, X. Piao, X. Jin, C.-S. Jon, L.u. Liu, J. Zhao, H.-B. Shang, D. Li, A reciprocating magnetic field assisted on-line solid-phase extraction coupled with liquid chromatography-tandem mass spectrometry determination of trace tetracyclines in water, Anal. Chim. Acta 1182 (2021) 338957.
[34] M. Mo, X. Wang, L. Ye, Y. Su, Y. Zhong, L. Zhao, Y. Zhou, J. Peng, A simple paper-based ratiometric luminescent sensor for tetracyclines using copper nanocluster-europium hybrid nanoprobes, Anal. Chim. Acta 1190 (2022), 339257, https://doi.org/10.1016/j.aca.2021.339257.
[35] H. Sereshti, G. Abdolhosseini, S. Soltani, F. Jamshidi, N. Nouri, Natural thymol-based ternary deep eutectic solvents: Application in air-bubble assisted-dispersive

liquid-liquid microextraction for the analysis of tetracyclines in water, J. Sep. Sci. 44 (2021) 3626–3635, https://doi.org/10.1002/jssc.202100495.

[36] J. Bengtsson-Palme, D.G.J. Larsson, Concentrations of antibiotics predicted to select for resistant bacteria: Proposed limits for environmental regulation, Environ. Int. 86 (2016) 140–149, https://doi.org/10.1016/j.envint.2015.10.015.

[37] Y. Jiang, M. Li, C. Guo, D. An, J. Xu, Y. Zhang, B. Xi, Distribution and ecological risk of antibiotics in a typical effluent–receiving river (Wangyang River) in north China, Chemosphere 112 (2014) 267–274, https://doi.org/10.1016/j.chemosphere.2014.04.075.